Electronic conductance of one-dimensional chains with phonon dephasing disorder

2006 J. Phys.: Condens. Matter 18 10059

(http://iopscience.iop.org/0953-8984/18/44/006)

INSTITUTE OF PHYSICS PUBLISHING JOURNAL OF PHYSICS: CONDENSED MATTER

J. Phys.: Condens. Matter **18** (2006) 10059–10073 doi:10.1088/0953-8984/18/44/006

Electronic conductance of one-dimensional chains with phonon dephasing disorder

A Cresti[1,2,3], **G Grosso**[1,2] **and G Pastori Parravicini**[1,4]

[1] NEST-CNR-INFM, Italy
[2] Dipartimento di Fisica 'E Fermi', Università di Pisa, Largo Pontecorvo 3, I-56127 Pisa, Italy
[3] Scuola Normale Superiore, Piazza dei Cavalieri 7, I-56126 Pisa, Italy
[4] Dipartimento di Fisica 'A Volta', Università di Pavia, Via A Bassi 6, I-27100 Pavia, Italy

E-mail: grosso@df.unipi.it

Received 4 August 2006, in final form 2 October 2006
Published 20 October 2006
Online at stacks.iop.org/JPhysCM/18/10059

Abstract

In this paper we analyse how electron transport through a one-dimensional chain is modified by the presence of phonon dephasing mechanisms active in a limited strand of the chain. The treatment is based on the nonequilibrium Keldysh Green's function and the self-consistent first Born approximation, with a tight-binding description of the electronic states. A most remarkable feature of the calculated conductance curves is the occurrence of an exponential decrease for small lengths, followed by a slow asymptotic decrease inversely proportional to the strand length. The origin of such a different short-range and long-range behaviour of the conductance, and other observed scaling features, are interpreted with some intuitive understanding of the dephasing mechanisms.

1. Introduction

Quantum transport through different nanostructures such as quantum dots, wires and molecular chains in the presence of phonon and other scattering mechanisms has been the object of an increasing amount of theoretical and experimental work aimed at understanding and controlling the electron flow in low-dimensional mesoscopic devices [1–3]. Recently the electron–phonon interaction in one-dimensional (1D) systems has become of fundamental interest mainly in connection with transport in molecular electronics [4, 5], carbon nanotubes [6], and organic and inorganic nanostructures [7]. Among the conceptual tools of interest concerning electron–phonon scattering is the insertion of inelastic scattering effects [8–12] in the Landauer–Büttiker theory [13, 14]. Scattering theory methods joined with iterative procedures have been applied to describe the transmission of electronic waves through disordered regions with phonon scattering [15–17].

The nonequilibrium Green's function formalism [18, 19] has become a very frequent and powerful approach to address the problem of conductance in the presence of electron–phonon interaction [20–23]. In fact, the nonequilibrium Keldysh formalism comprises the full many-body quantum theory [24]; it describes the scattering mechanisms (electron–phonon, electron–electron, or others) by appropriate self-energy operators, which can be derived systematically from many-body perturbation theory. In particular the self-consistent Born approximation [21, 22, 25, 26] has been widely applied, because it is still reasonably simple computationally although it goes beyond first order and actually entails a partial summation of the perturbation series; furthermore, and most importantly, the condition of current conservation is automatically encompassed [26].

Strictly 1D or almost 1D systems have been generally adopted for about half a century in the theoretical study of disorder, since the pioneering work of Anderson [27]. The usual approach is to consider a 1D strand composed of N sites, belonging to an infinite linear chain, in which models of disorder are introduced, and to evaluate the localization length of the electronic states [28]. This is often achieved via numerical treatments which mostly rely on the evaluation of conductance (or of localization length) with transfer matrix techniques or diagrammatic expansions, starting from the Hamiltonian corresponding to a disordered configuration of the system, and then performing averages on a sufficiently high number of configurations. It should be noticed that, within the self-consistent first Born approximation, the disorder averaging procedure is embodied in the formalism once the self-consistent calculations of the retarded (advanced) and lesser (greater) self-energies for electron–phonon scattering have been carried out and appropriately elaborated.

In this work we shall use the self-consistent Born approximation for a systematic study of phonon dephasing disorder on a strand of an otherwise periodic infinite linear chain. The conductance through the devices is elaborated in terms of the coherent and incoherent contributions corresponding to carriers that tunnel without or with the assistance of phonon scattering processes, respectively. The underlying principle for such separation emerges naturally from the exact self-consistent account of the full set of retarded, advanced, lesser and greater phonon self-energies and electron Green's functions. Closed expressions for the coherent and incoherent contributions to the total conductance are obtained; their behaviour as a function of the sample length and disorder strength is provided numerically. Most importantly, some features of conductance can be inferred from the structure of the formalism, and this helps a better intuitive understanding of phonon dephasing effects.

In section 2 we describe the system and the model Hamiltonian for the disordered strand coupled to perfect leads. The Keldysh expression of the current in the presence of scattering mechanisms is briefly outlined. In section 3 we analyse the electron–phonon coupling in the tight-binding representation for the electronic states; the phonon self-energies are expressed within the Born self-consistent approximation and worked out in terms of corresponding electronic propagators. In section 4 the analytic expressions for the coherent and incoherent contributions to the transmission coefficient are provided. The exact self-consistent calculation of the retarded (advanced) phonon self-energies $\Sigma^{R,A(\mathrm{ph})}$ is achieved by means of a continued fraction expansion, which benefits from a rapid convergence. The exact self-consistent calculation of the lesser (greater) phonon self-energies $\Sigma^{<,>(\mathrm{ph})}$ is achieved by elaborating the Keldysh kinetic equations into an appropriate set of linear non-homogeneous equations, that are then solved with standard routines. In either case, the rank of the matrices to be handled is restricted to the number of sites of the central device in consideration. In section 5 numerical simulations of conductance versus device length and electron–phonon coupling are obtained and corroborated by intuitive insights which allow a sound understanding of phonon dephasing mechanisms. The conclusions are reported in section 6.

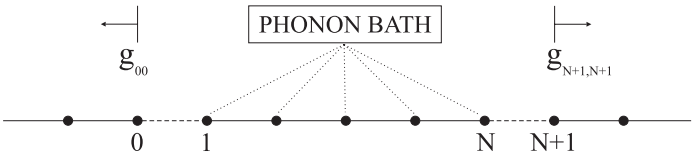

Figure 1. Typical arrangement for the analysis of electron transport in a 1D quantum wire. The box denotes a phonon bath at thermodynamic equilibrium; the dotted lines represent local phonon scattering processes in the central device.

2. System description and tunnelling current

We consider a strand of a 1D chain with internal scattering due to electron–phonon coupling. The remaining parts of the chain act as perfect leads connected to the left and right reservoirs at different chemical potentials. The electronic part of the complete system is described in the tight-binding framework, with a single orbital per site. The model electron-plus-phonon Hamiltonian can be written in the form

$$H = H_{\rm e} + H_{\rm p} + H_{\rm ep}, \tag{1}$$

where $H_{\rm e}$ is the one-body Hamiltonian of the perfect chain, $H_{\rm p}$ is the one-body Hamiltonian of the phonon modes, and $H_{\rm ep}$ is the electron–phonon coupling. The electron Hamiltonian is usually split in the form (see figure 1)

$$H_{\rm e} = H_0^{(\rm left)} + H_0^{(D)} + H_0^{(\rm right)} + W_{\rm coupl}; \tag{2}$$

the first three terms describe the left lead, central strand, and right lead, disconnected from each other, and $W_{\rm coupl}$ couples the central device and the leads. As usual, it is assumed that the interaction of phonon and electron operators is confined to the central device, and leads are free from scattering mechanisms. The central region extends from site 1 to site N.

The phonon scattering effects are described by the retarded, advanced, lesser and greater self-energy operators $\Sigma^{A(\rm ph)}$, $\Sigma^{R(\rm ph)}$, $\Sigma^{<(\rm ph)}$, $\Sigma^{>(\rm ph)}$; in the next section we show how to determine them, within the self-consistent Born approximation. The self-energy operators $\Sigma^{A,R,>,<(\rm leads)}$ describe the coupling of the central device to the leads. For the leads, and for the strand not yet in contact with leads and with the phonon bath, we denote the electronic Green's functions as g^R, g^A, $g^>$, $g^<$; the occupation Fermi functions of the left and of the right leads (initially at equilibrium) are denoted by $f_{\rm L}(E)$ and $f_{\rm R}(E)$, and the corresponding chemical potentials are $\mu_{\rm L}$ and $\mu_{\rm R}$.

When the couplings of the strand with the leads and with phonons are switched on, the kinetic equation for the lesser Green's function of the strand provided by the Keldysh theory reads [22, 29]

$$G^< = G^R \Sigma^{<(\rm leads)} G^A + G^R\, \Sigma^{<(\rm ph)} G^A \qquad (i, j = 1, 2, \ldots, N). \tag{3}$$

The self-energies due to the effect of the open leads on the central region are conveniently described in terms of the so-called 'escape rate matrices', or 'broadening operators', as follows:

$$\Sigma_{11}^{<(\rm left)} = {\rm i} f_{\rm L} \Gamma_{11}^{(\rm left)}; \qquad \Sigma_{NN}^{<(\rm right)} = {\rm i} f_{\rm R} \Gamma_{NN}^{(\rm right)} \tag{4}$$

with

$$\Gamma_{11}^{(\rm left)} = {\rm i} t_{10} (g_{00}^R - g_{00}^A) t_{01} = {\rm i}[\Sigma_{11}^{R(\rm left)} - \Sigma_{11}^{A(\rm left)}]$$
$$\Gamma_{NN}^{(\rm right)} = {\rm i} t_{N,N+1} (g_{N+1,N+1}^R - g_{N+1,N+1}^A) t_{N+1,N} = {\rm i}[\Sigma_{NN}^{R(\rm right)} - \Sigma_{NN}^{A(\rm right)}].$$

In the above expressions t_{ij} are the nearest-neighbour interactions between site i and site j. In the following we shall assume for simplicity that all nearest-neighbour hopping parameters equal t, and $|t|$ will be taken as the unit of energy. From equation (3) we have in particular that the nonequilibrium lesser Green's function on the initial site of the strand is

$$G^<_{11} = [G^R \Sigma^{<(\text{leads})} G^A]_{11} + [G^R \Sigma^{<(\text{ph})} G^A]_{11}; \tag{5}$$

in the literature the two terms are commonly referred to as 'coherent' and 'incoherent' for reasons that will become apparent soon. We now have all the ingredients to express the current through the 1D device of figure 1.

The current crossing the bond from site 0 to site 1 in steady state conditions is given by the expression [29]

$$I = \frac{2(-e)}{\hbar} \int \frac{\mathrm{d}E}{2\pi} \left[t_{01} G^<_{10} - t_{10} G^<_{01} \right], \tag{6}$$

where the factor 2 takes into account the spin degeneracy. By virtue of the relations

$$G^<_{01} = g^R_{00} t_{01} G^<_{11} + g^<_{00} t_{01} G^A_{11}$$

and

$$G^<_{10} = G^R_{11} t_{10} g^<_{00} + G^<_{11} t_{10} g^A_{00},$$

equation (6) can be cast in the equivalent form

$$I = \frac{-2e}{\hbar} \int \frac{\mathrm{d}E}{2\pi} \left[\Sigma^{<(\text{left})}_{11} G^>_{11} - \Sigma^{>(\text{left})}_{11} G^<_{11} \right]. \tag{7}$$

Inserting equation (5) into (7) we obtain that the current can be split into a 'coherent part' (whose origin is traced back to the leads' lesser self-energies) and an 'incoherent part' (whose origin is traced back to the phonons' lesser self-energies) as follows:

$$I = I_{\text{coh}} + I_{\text{inc}}, \tag{8a}$$

with

$$I_{\text{coh}} = \frac{-2e}{\hbar} \int \frac{\mathrm{d}E}{2\pi} \left[\Sigma^{<(\text{left})}_{11} \left(G^R \Sigma^{>(\text{leads})} G^A \right)_{11} - \Sigma^{>(\text{left})}_{11} \left(G^R \Sigma^{<(\text{leads})} G^A \right)_{11} \right], \tag{8b}$$

and

$$I_{\text{inc}} = \frac{-2e}{\hbar} \int \frac{\mathrm{d}E}{2\pi} \left[\Sigma^{<(\text{left})}_{11} \left(G^R \Sigma^{>(\text{ph})} G^A \right)_{11} - \Sigma^{>(\text{left})}_{11} \left(G^R \Sigma^{<(\text{ph})} G^A \right)_{11} \right]. \tag{8c}$$

Using equations (4), the coherent contribution can also be written in the more familiar form:

$$I_{\text{coh}} = \frac{-2e}{\hbar} \int \frac{\mathrm{d}E}{2\pi} \left(f_{\text{L}} - f_{\text{R}} \right) \Gamma^{(\text{left})}_{11} G^R_{1N} \Gamma^{(\text{right})}_{NN} G^A_{N1}. \tag{8d}$$

Notice that both $\Sigma^{R,A(\text{leads})}$ and $\Sigma^{R,A(\text{ph})}$ (these latter to be determined self-consistently) are required for the determination of $G^{R,A}$; furthermore $\Sigma^{<,>(\text{leads})}$ and $\Sigma^{<,>(\text{ph})}$ (these latter to be determined self-consistently) are also required for the determination of $G^{<,>}$. It is also well known that the rigorous formulation of the self-consistent Born framework, and the exact numerical evaluation, are both mandatory to guarantee current conservation and make possible a sound physical interpretation of the numeric simulations.

3. Phonon self-energy model in the high-temperature limit

We consider the usual expression for the electron–phonon interaction in terms of electronic $(c_i^\dagger, c_i)$ and bosonic $(b_k^\dagger, b_k)$ creation and annihilation operators:

$$H_{\rm ep} = \sum_{ijk} M_{ijk} c_i^\dagger c_j u_k \tag{9}$$

with $u_k = (b_k + b_{-k}^\dagger)$. In the following we shall adopt the local dephasing model in which the localization of phonons is so strong to allow us to restrict their effect within each single site [21, 22]. Thus the electron–phonon coupling can be approximated as composed by single site terms of the type

$$H_{\rm ep}^{(i)} = M_i c_i^\dagger c_i u_i. \tag{10}$$

For simplicity, we also assume site-independent parameters M, and a single phonon of frequency Ω_0 for the energy spectrum of the local oscillators.

In applying the Keldysh theory, the thermal average is performed independently for the Fermi gas and the thermal bath of phonons. The phonon self-energy at the lowest order of approximation (known as Fock diagram, in analogy to the electron many-body problem) is given by (see for instance [22])

$$\Sigma_{ii}^{(K)(ph)}(\tau, \tau') = \mathrm{i}\hbar M^2 D_{ii}^{(K)}(\tau, \tau') G_{ii}^{(K)}(\tau, \tau'). \tag{11}$$

The time variables (τ, τ') run along the Keldysh contour where phonon $(D^{(K)})$ and electron $(G^{(K)})$ propagators are evaluated. Exploiting the Langreth rules [30] to handle products of phonon and electron propagators, and performing the Fourier transform, we obtain the expressions [25]

$$\begin{aligned}
\Sigma_{ii}^{R(\rm ph)}(\hbar\omega) &= \mathrm{i}M^2 \int \frac{\mathrm{d}\epsilon}{2\pi} \left[D^R(\hbar\omega - \epsilon) G_{ii}^<(\epsilon) + D^>(\hbar\omega - \epsilon) G_{ii}^R(\epsilon) \right] \\
\Sigma_{ii}^{<(\rm ph)}(\hbar\omega) &= \mathrm{i}M^2 \int \frac{\mathrm{d}\epsilon}{2\pi} D^<(\hbar\omega - \epsilon) G_{ii}^<(\epsilon) \\
\Sigma_{ii}^{>(\rm ph)}(\hbar\omega) &= \mathrm{i}M^2 \int \frac{\mathrm{d}\epsilon}{2\pi} D^>(\hbar\omega - \epsilon) G_{ii}^>(\epsilon) \\
\Sigma_{ii}^{A(\rm ph)}(\hbar\omega) &= \mathrm{i}M^2 \int \frac{\mathrm{d}\epsilon}{2\pi} \left[D^A(\hbar\omega - \epsilon) G_{ii}^<(\epsilon) + D^>(\hbar\omega - \epsilon) G_{ii}^A(\epsilon) \right],
\end{aligned}$$

where $D^{R,A,<,>}$ are the retarded, advanced, lesser and greater free-phonon Green's functions. These are given by the expressions

$$\begin{aligned}
D^<(E) &= -2\pi\mathrm{i}\left[(n_0 + 1)\delta(E + \hbar\Omega_0) + n_0\delta(E - \hbar\Omega_0)\right] \\
D^>(E) &= -2\pi\mathrm{i}\left[(n_0 + 1)\,\delta(E - \hbar\Omega_0) + n_0\delta(E + \hbar\Omega_0)\right] \\
D^R(E) &= \frac{1}{E - \hbar\Omega_0 + \mathrm{i}\eta} - \frac{1}{E + \hbar\Omega_0 + \mathrm{i}\eta} \\
D^A(E) &= \frac{1}{E - \hbar\Omega_0 - \mathrm{i}\eta} - \frac{1}{E + \hbar\Omega_0 - \mathrm{i}\eta},
\end{aligned}$$

where n_0 is the occupation number for the phonon of frequency Ω_0.

In the limit of high phonon-occupation number ($\hbar\Omega_0 \ll k_{\rm B}T$), the above relations give

$$D^R(E) \approx D^A(E) \ll D^<(E) \approx D^>(E), \tag{12}$$

and the expressions for the phonon self-energies are greatly simplified since we can neglect retarded and advanced phonon Green's functions with respect to the lesser and greater

functions, and we can also replace the greater Green's function with the lesser one. We then have

$$\Sigma_{ii}^{R,A,<,>(\mathrm{ph})}(E) = \mathrm{i}M^2 \int \frac{\mathrm{d}\epsilon}{2\pi} D^{<}(\epsilon) G_{ii}^{R,A,<,>}(E-\epsilon). \tag{13}$$

Thus in the high-occupancy limit, each phonon self-energy is related to the corresponding electron Green's function through the same linear functional (as shown by Klimeck *et al* [22] and Ratner *et al* [5]). This approximation greatly simplifies the Keldysh equations.

From equation (13) and the expression of the lesser phonon Green's functions $D^{<}$, it is seen that the phonon self-energies in the self-consistent Born approximation can be expressed as

$$\Sigma_{ii}^{R,A,<,>(\mathrm{ph})}(E) = M^2 \left[(n_0+1) G_{ii}^{R,A,<,>}(E+\hbar\Omega_0) + n_0 G_{ii}^{R,A,<,>}(E-\hbar\Omega_0) \right]$$

where M is the electron–phonon coupling, and $n_0 \approx k_\mathrm{B}T/\hbar\Omega_0 \gg 1$ is the phonon occupation number in the limit of phonon energy sufficiently small with respect to the thermal energy $k_\mathrm{B}T$. If the electron properties and Green's functions are slowly varying in the energy domain with respect to the phonon energy $\hbar\Omega_0$, we can simplify the above equation in the form

$$\Sigma_{ii}^{R,A,<,>(\mathrm{ph})}(E) = \gamma^2 G_{ii}^{R,A,<,>}(E) \qquad (i = 1, 2, \ldots, N), \tag{14}$$

where the expression of the parameter γ as a function of temperature, phonon frequency and electron–phonon interaction, within the stated approximations, is

$$\gamma = M^2(2n_0+1) \approx 2M^2 \frac{k_\mathrm{B}T}{\hbar\Omega_0}.$$

The positive parameter γ has the dimension of energy, and expresses the effective dephasing constant due to the coupling between the phonon field and the fermion field; for simplicity the parameter γ is taken independent from the site; the case of site-dependent γ_i can be treated similarly. Before closing, we wish to note that the adopted dephasing model local both in energy and space, and summarized by equation (14), is of value not only in the present context of electron–phonon interaction, but also in other models of dephasing mechanisms concerning, for instance, alloy disorder effects, interface roughness, and impurity ensemble averages [22].

4. Currents through mesoscopic one-dimensional systems and dephasing effects

4.1. Green's functions and self-energy operators for phonon dephasing

We consider now how the current through a 1D system is modified by the presence of dephasing in its central region extending from site 1 to site N; the values of N actually considered vary from several tens to a few thousands, as needed in the specific situations. The retarded Green's function in the central device becomes

$$\begin{aligned} G^R(E) &= \frac{1}{E - H_0^{(D)} - \Sigma^{R(\mathrm{leads})}(E) - \Sigma^{R(\mathrm{ph})}(E)} \\ &= \frac{1}{E - H_0^{(D)} - \Sigma^{R(\mathrm{leads})}(E) - \gamma^2 \mathcal{D} G^R(E)} \qquad (i, j = 1, 2, \ldots, N), \end{aligned} \tag{15}$$

where equation (14) has been used, and $\mathcal{D}$ denotes the superoperator that picks up the diagonal part of the matrix following it. The solution of the above equation can be expressed in the matrix continued fraction form:

$$G^R(E) = \cfrac{1}{E - H_0^{(D)} - \Sigma^{R(\mathrm{leads})} - \gamma^2 \mathcal{D} \cfrac{1}{E - H_0^{(D)} - \Sigma^{R(\mathrm{leads})} - \gamma^2 \mathcal{D} \frac{1}{E - \cdots}}}. \tag{16}$$

All the matrices in the above equation are restricted to the N sites of the central strand, and have rank N. Since the Green's function $G^R(E) = [E - H_0^{(D)} - \Sigma^{R(\text{leads})}(E)]^{-1}$ is known analytically (in the case of linear chain with constant diagonal and nearest-neighbour interactions) or numerically (for more complicated models), the continued fraction (16) can be evaluated at arbitrary order until necessary.

In the numerical simulations presented in this paper, a satisfactory convergence of the continued fraction expansion was usually achieved within about ten steps or so. The fast convergence and the analytic properties of the continued fraction apparatus are at the basis of its wide application in several fields, including equilibrium electronic properties of materials [31], vibronic and Jahn–Teller systems [32], and quantum transport in coupled electronic-vibrational devices [22].

The calculation of equation (16) permits the knowledge of the retarded Green's function on the central device, and hence of phonon retarded self-energies according to equation (14). From the knowledge of G^R, G^A, $\Sigma^{R(\text{ph})}$, $\Sigma^{A(\text{ph})}$ we can now pass to the evaluation of the lesser (or greater) Green's function. Using equations (14) and (3), we obtain

$$\Sigma_{jj}^{<(\text{ph})}(E) = \gamma^2 \left[G^R \Sigma^{<(\text{leads})} G^A + G^R \Sigma^{<(\text{ph})} G^A \right]_{jj}; \tag{17}$$

or more explicitly

$$\Sigma_{jj}^{<(\text{ph})}(E) = \gamma^2 [G^R \Sigma^{<(\text{leads})} G^A]_{jj} + \gamma^2 \sum_{\nu} G_{j\nu}^R \Sigma_{\nu\nu}^{<(\text{ph})} G_{\nu j}^A \qquad (j, \nu = 1, 2, \ldots, N). \tag{18}$$

For the elaboration of the above expressions, it is convenient to introduce two vectors, $\mathbf{X}$ and $\mathbf{V}$, and a matrix Q (the dimensions of the vectors and the rank of the matrix are equal to the number N of sites of the central device) defined as follows:

$$X_j = \Sigma_{jj}^{<(\text{ph})}, \qquad V_j = [G^R \Sigma^{<(\text{leads})} G^A]_{jj}, \qquad Q_{j\nu} = G_{j\nu}^R G_{\nu j}^A \equiv |G_{j\nu}^R|^2. \tag{19}$$

The set of equations (18) can be cast in the compact form

$$\mathbf{X} = \gamma^2 \mathbf{V} + \gamma^2 Q \mathbf{X};$$

the solution is

$$\mathbf{X} = Z\mathbf{V} \qquad \text{with } Z = \gamma^2 \frac{1}{1 - \gamma^2 Q}. \tag{20}$$

The explicit expression of the lesser self-energy reads

$$\begin{aligned} \Sigma_{jj}^{<(\text{ph})}(E) &= \sum_{\nu} Z_{j\nu} V_\nu = \sum_{\nu} Z_{j\nu} \left[G^R \Sigma^{<(\text{leads})} G^A \right]_{\nu\nu} \\ &= \sum_{\nu} Z_{j\nu} \left[G^R \Sigma^{<(\text{left})} G^A \right]_{\nu\nu} + \sum_{\nu} Z_{j\nu} \left[G^R \Sigma^{<(\text{right})} G^A \right]_{\nu\nu} \\ &= \mathrm{i} f_{\text{L}} \sum_{\nu} Z_{j\nu} \left[G^R \Gamma^{(\text{left})} G^A \right]_{\nu\nu} + \mathrm{i} f_{\text{R}} \sum_{\nu} Z_{j\nu} \left[G^R \Gamma^{(\text{right})} G^A \right]_{\nu\nu}. \end{aligned} \tag{21}$$

The first term in the last line can be elaborated in a more compact form as follows:

$$\sum_{\nu} Z_{j\nu} \left[G^R \Gamma^{(\text{left})} G^A \right]_{\nu\nu} = \sum_{\nu} Z_{j\nu} G_{\nu 1}^R \Gamma_{11}^{(\text{left})} G_{1\nu}^A = \sum_{\nu} Z_{j\nu} Q_{\nu 1} \Gamma_{11}^{(\text{left})} = [ZQ]_{j1} \Gamma_{11}^{(\text{left})};$$

a similar treatment can be done on the other term.

Introducing the auxiliary matrix

$$A = ZQ = \gamma^2 \frac{Q}{1 - \gamma^2 Q}, \tag{22}$$

we have the following result:

$$\Sigma_{jj}^{<(\text{ph})} = \mathrm{i} f_{\text{L}} A_{j1} \Gamma_{11}^{(\text{left})} + \mathrm{i} f_{\text{R}} A_{jN} \Gamma_{NN}^{(\text{right})} \qquad j = 1, 2, \ldots, N. \tag{23}$$

We are now in a position to calculate the matrix element $[G^R\Sigma^{<(\mathrm{ph})}G^A]_{11}$ that enters into the current equation (8*c*). We have

$$\begin{aligned}[G^R\Sigma^{<(\mathrm{ph})}G^A]_{11} &= \sum_j G^R_{1j}\Sigma^{<(\mathrm{ph})}_{jj}G^A_{j1} \\ &= \sum_j Q_{1j}\left[\mathrm{i}f_{\mathrm{L}}A_{j1}\Gamma^{(\mathrm{left})}_{11} + \mathrm{i}f_{\mathrm{R}}A_{jN}\Gamma^{(\mathrm{right})}_{NN}\right] \\ &= \mathrm{i}f_{\mathrm{L}}B_{11}\Gamma^{(\mathrm{left})}_{11} + \mathrm{i}f_{\mathrm{R}}B_{1N}\Gamma^{(\mathrm{right})}_{NN}, \end{aligned} \tag{24}$$

where the auxiliary B matrix is defined as

$$B = QA = \gamma^2\frac{Q^2}{1-\gamma^2 Q}. \tag{25}$$

Similarly, we have

$$[G^R\Sigma^{>(\mathrm{ph})}G^A]_{11} = -\mathrm{i}(1-f_{\mathrm{L}})B_{11}\Gamma^{(\mathrm{left})}_{11} - \mathrm{i}(1-f_{\mathrm{R}})B_{1N}\Gamma^{(\mathrm{right})}_{NN}.$$

We now have all the ingredients for the calculation of the effect of dephasing on the current flow in 1D mesoscopic systems.

4.2. Dephasing effects on the electronic conductance and the transmission coefficient

Introducing the results of the previous subsection in expressions (8) for the currents, we obtain

$$I = I_{\mathrm{coh}} + I_{\mathrm{inc}} \tag{26a}$$

with

$$I_{\mathrm{coh}} = \frac{-2e}{h}\int \mathrm{d}E(f_{\mathrm{L}} - f_{\mathrm{R}})\Gamma^{(\mathrm{left})}_{11}Q_{1N}\Gamma^{(\mathrm{right})}_{NN} \tag{26b}$$

$$I_{\mathrm{inc}} = \frac{-2e}{h}\int \mathrm{d}E(f_{\mathrm{L}} - f_{\mathrm{R}})\Gamma^{(\mathrm{left})}_{11}B_{1N}\Gamma^{(\mathrm{right})}_{NN}, \tag{26c}$$

where Q and B are matrices of rank N, already defined. In the limiting situation that the chemical potentials of the left reservoir and of the right reservoir are very near to each other (linear response regime), equations (26) take the approximate form

$$I_{\mathrm{coh}} = \frac{-2e}{h}(\mu_{\mathrm{L}} - \mu_{\mathrm{R}})\Gamma^{(\mathrm{left})}_{11}Q_{1N}\Gamma^{(\mathrm{right})}_{NN}$$

$$I_{\mathrm{inc}} = \frac{-2e}{h}(\mu_{\mathrm{L}} - \mu_{\mathrm{R}})\Gamma^{(\mathrm{left})}_{11}B_{1N}\Gamma^{(\mathrm{right})}_{NN}.$$

From the above equations, we can split the total transmission coefficient into the coherent and noncoherent contributions as follows:

$$T(E) = T_{\mathrm{coh}}(E) + T_{\mathrm{inc}}(E) \tag{27a}$$

with

$$T_{\mathrm{coh}}(E) = \Gamma^{(\mathrm{left})}_{11}Q_{1N}\Gamma^{(\mathrm{right})}_{NN} \tag{27b}$$

$$T_{\mathrm{inc}}(E) = \Gamma^{(\mathrm{left})}_{11}B_{1N}\Gamma^{(\mathrm{right})}_{NN}. \tag{27c}$$

Equations (27) also express the (differential) conductance in units of $2e^2/h$ at the electronic Fermi energy E.

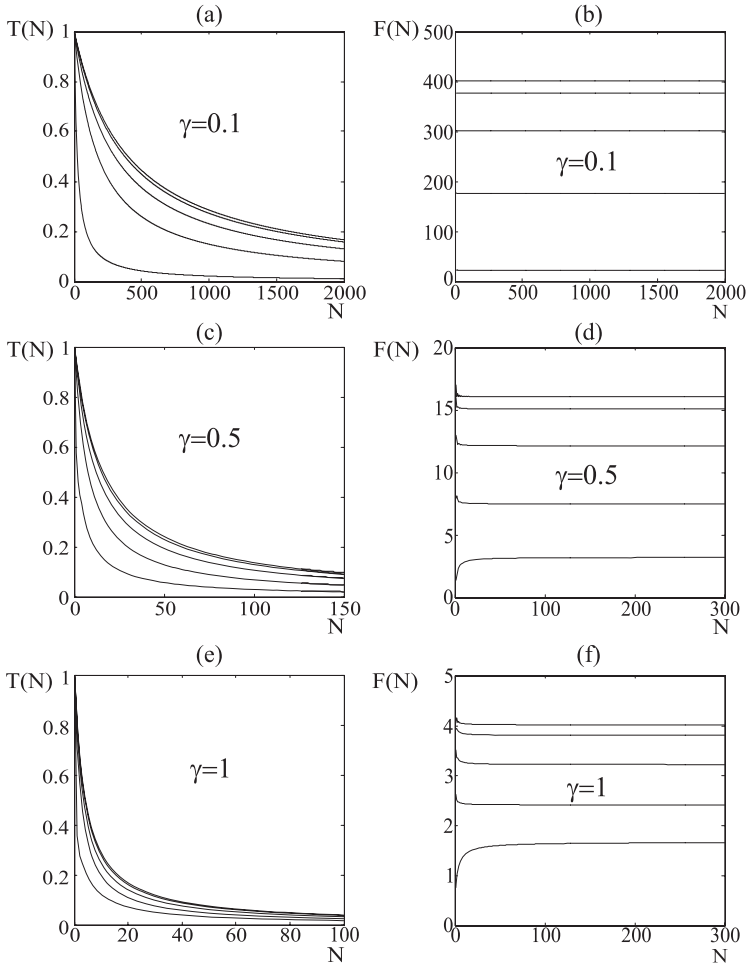

Figure 2. Total transmission coefficient $T(N)$ for different energies ($E = 0, 0.5, 1, 1.5, 1.95$) and coupling parameter $\gamma = 0.1$ (a), $\gamma = 0.5$ (c) and $\gamma = 1$ (e). Plot of the quantity $F(N) = NT(N)/[1 - T(N)]$ at the same energies and coupling parameters.

5. Numerical results and discussion

We present in this section a detailed numerical analysis of the phonon dephasing effects on the conductance of a 1D system for different values of the central device length, electron–phonon coupling constants and Fermi energies. If not specified otherwise, the unit of length is the lattice parameter a, the unit of energy is the modulus $|t|$ of the nearest-neighbour hopping parameter, the unit of conductance is $2e^2/h$, and the unit of resistance is $h/2e^2$. As observed in the previous section, the first step of our numerical procedure is the exact self-consistent calculation of the retarded (advanced) Green's function, given by the rapidly convergent continued fraction expression (16). From the matrix Q and the auxiliary matrix B contributions equations (27) are then evaluated.

The total transmission coefficient $T(N)$ as a function of the strand length N is reported in figure 2. Figures 2(a), (c), (e) refer to the electron–phonon parameter $\gamma = 0.1$, $\gamma = 0.5$, and $\gamma = 1$, respectively. For all the cases, the transmission coefficients are calculated at the

energies $E = 0$, 0.5, 1, 1.5 and 1.95 (in units of $|t|$). From the numerical results of figure 2 we can infer the phase relaxation lengths with the following considerations. The resistance of an array of scatterers is expected to increase linearly with the length of the array ('ohmic behaviour'), if the interference effects between successive arrays of scatterers can be neglected. In the ohmic regime, the transmission probability assumes the typical behaviour

$$T(N) = \frac{N_0}{N + N_0}, \tag{28}$$

and $L_0 = N_0 a$ characterizes the phase relaxation length introduced by the dephasing mechanism. The validity of equation (28) entails that the resistance (in units of $h/2e^2$) of the central 1D device increases linearly with its length in agreement with Ohm's law:

$$R(N) = \frac{1 - T(N)}{T(N)} = \frac{N}{N_0}. \tag{29}$$

To verify the ohmic behaviour of the chosen device for large values of $L = Na$, from the data for $T(N)$ reported in figure 2, we plot the quantity

$$F(N) = N\frac{T(N)}{1 - T(N)}$$

as function of N. From figures 2(b), (d), (f) it is evident that $F(N)$ becomes constant for sufficiently large values of N; the asymptotic values represent the dephasing lengths (in units of a).

A detailed analysis of our data for the dephasing lengths N_0 for several coupling strengths, suggests the following trend:

$$N_0 = \frac{\alpha(E)}{\gamma^2},$$

where $\alpha(E)$ is (almost) independent of the parameter γ (at least for energies not too close to the band edges $E = \pm 2|t|$). For instance, from figures 2(b), (d), (f) it is seen that, at the energy $E = 0$, we have $N_0 \approx 400$ for $\gamma = 0.1$, $N_0 \approx 16$ for $\gamma = 0.5$ and $N_0 \approx 4$ for $\gamma = 1$. The numerical values of the transmission probability $T(N)$ can be fitted for sufficiently large N by a one-parameter scaling function of the type

$$T(N) \approx \frac{1}{1 + N/N_0} = g\left(\frac{N}{N_0}\right), \tag{30}$$

where $g(x)$ is the algebraic expression $g(x) = 1/(1 + x)$.

Figure 3 shows the coherent and incoherent components of the conductance in the same cases considered in figure 2. We notice that the coherent term decreases rapidly from unity to zero as N increases. In contrast, the incoherent term increases linearly with N for small N until it becomes the dominant contribution to the conductance; then it decreases slowly to zero. The analysis of several different coupling strengths γ and lengths N shows that the logarithm of the coherent contribution can be accurately fitted by straight lines as shown in figures 3(b), (d) and (f); this indicates an exponential decay law of the type

$$T_{\text{coh}} = \exp\left[-\gamma^2 N/\beta(E)\right], \tag{31}$$

where $\beta(E)$ depends on the energy E, but is (almost) independent of the coupling strength γ and of the length N (at least for energies E not too close to the band edges).

In summary, the coherent contribution can be fitted (except near the band edges) by a one-parameter scaling function of the type

$$T_{\text{coh}} = \exp\left[-L/\xi\right] \qquad \text{with } \xi = \frac{\beta(E)}{\gamma^2}a. \tag{32}$$

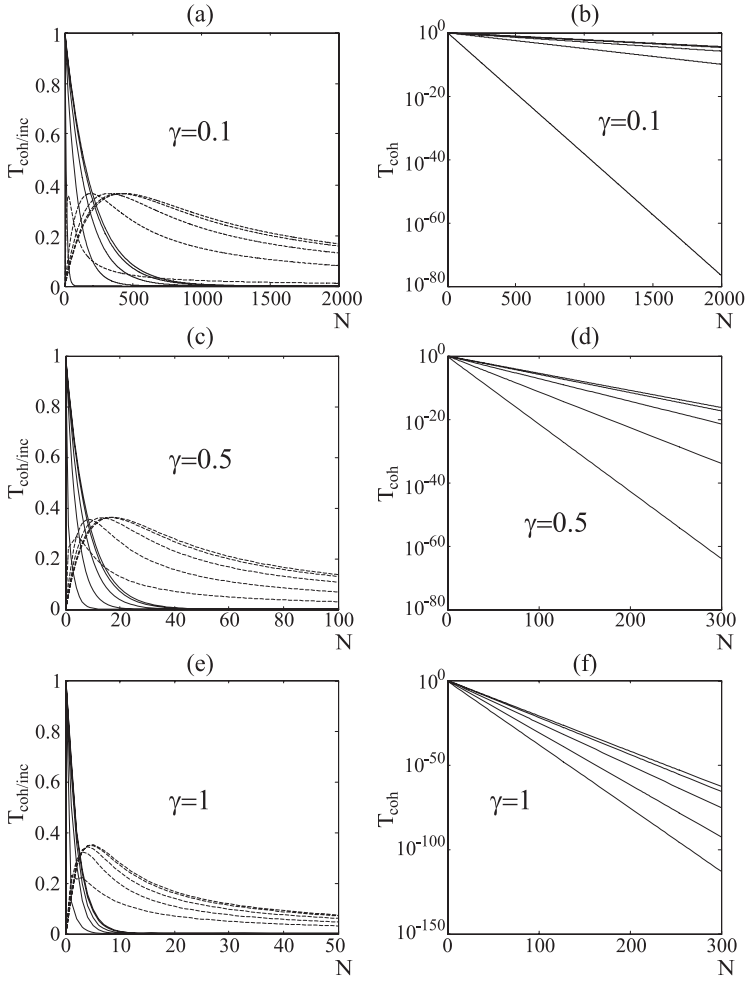

Figure 3. Coherent (solid lines) and incoherent (dotted lines) transmission components for $\gamma = 0.1$ (a), $\gamma = 0.5$ (c) and $\gamma = 1$ (d). In (b), (d) and (f) the coherent components are reported in a semilogarithmic scale, evidencing their exponential decaying.

This should be contrasted with the asymptotic contribution of the incoherent term which can be fitted for sufficiently large N by one parameter scaling function of the type

$$T_{\rm inc} \approx \frac{L_0}{L_0 + L} \qquad \text{with } L_0 = \frac{\alpha(E)}{\gamma^2} a. \tag{33}$$

While the scaling behaviour of the coherent term hints at exponential localization of electronic wavefunctions, the algebraic scaling behaviour of the incoherent term represents a peculiar and systematic feature in all the present calculations. Because of the importance of this term, whose possible role in polymer and molecular electronics has recently received attention [5], we perform some further numerical and analytic analysis to clarify its origin.

For an ideally periodic 1D chain with site energies equal to $E_0 = 0$ and nearest-neighbour hopping parameter t (<0), the retarded Green's function between sites m and n, at energies

within the energy band, has the analytic expression [33]

$$G^R_{mn}(E) = \frac{\mathrm{e}^{-\mathrm{i}\phi(E)|m-n|}}{2\mathrm{i}|t|\sin\phi} \qquad -2|t| < E < +2|t| \tag{34a}$$

and

$$\phi(E) = \arccos\frac{E}{2t} \qquad \text{with } 0 < \phi < \pi. \tag{34b}$$

In the absence of scattering, the Q-matrix elements of the strand take the simplified form

$$Q_{mn} = \left|G^R_{mn}\right|^2 = Q_{11};$$

in other words, the diagonal and off-diagonal matrix elements of Q are equal.

In the presence of dephasing, the phonon self-energy $\Sigma^{R(\mathrm{ph})}_{jj}$ in the central strand enters (self-consistently) into the determination of the retarded electron propagator. Assuming the length of the central strand to be sufficiently wide so that the $\Sigma^{R(\mathrm{ph})}_{jj}$ is site independent (at least in the bulk of the device), we can write the Green's function as

$$G^R_{mn}(E) = \frac{\mathrm{e}^{-\mathrm{i}\phi_c(E)|m-n|}}{2\mathrm{i}|t|\sin\phi_c} \tag{35a}$$

where

$$\phi_c(E) = \arccos\frac{E - \Sigma^{R(\mathrm{ph})}}{2t} \tag{35b}$$

is now a complex quantity. In the weak (or intermediate) dephasing limit, we expect $\Sigma^{R(\mathrm{ph})} \approx -\mathrm{i}\gamma^2/2|t| < 1$. A series development of equation (35*b*) gives for the real and imaginary part of ϕ_c the expression

$$\mathrm{Re}\,\phi_c(E) = \phi(E) \qquad \text{and} \qquad \mathrm{Im}\;\phi_c(E) = -\frac{\gamma^2}{2c(E)} \qquad \text{with}$$

$$c(E) = \frac{1}{|t|\sqrt{4t^2 - E^2}} > 0.$$

We thus recover for the matrix Q the decreasing exponential behaviour

$$Q_{mn} = Q_{11}\mathrm{e}^{-\gamma^2|m-n|/c(E)},$$

which is in agreement with the scaling behaviour (31) observed numerically and with equation (27*b*). In the strong dephasing limit, we have $\Sigma^{R(\mathrm{ph})} \approx -\mathrm{i}\gamma$ and similar considerations can be worked out.

The above qualitative remarks on the Q-matrix explain the feature of the coherent contribution to the conductance behaviour. We have already noted that, in order to satisfy current conservation, it is not possible to consider only the retarded (and advanced) phonon self-energy (in a kind of purely 'optical potential' point of view), and it is necessary to account properly for the lesser (and greater) phonon self-energy. Actually, these quantities in the Keldysh theory are linked in a unique destiny, and in particular by the relation $\Sigma^{>(\mathrm{ph})} - \Sigma^{<(\mathrm{ph})} = \Sigma^{R(\mathrm{ph})} - \Sigma^{A(\mathrm{ph})}$; thus it is not possible to account for $\Sigma^{R,A(\mathrm{ph})}$ and neglect $\Sigma^{<,>(\mathrm{ph})}$, without violating current conservation.

As regards the incoherent transmission of equation (27*c*), the relevant term is given by the matrix

$$B = \gamma^2\frac{Q^2}{1 - \gamma^2 Q}.$$

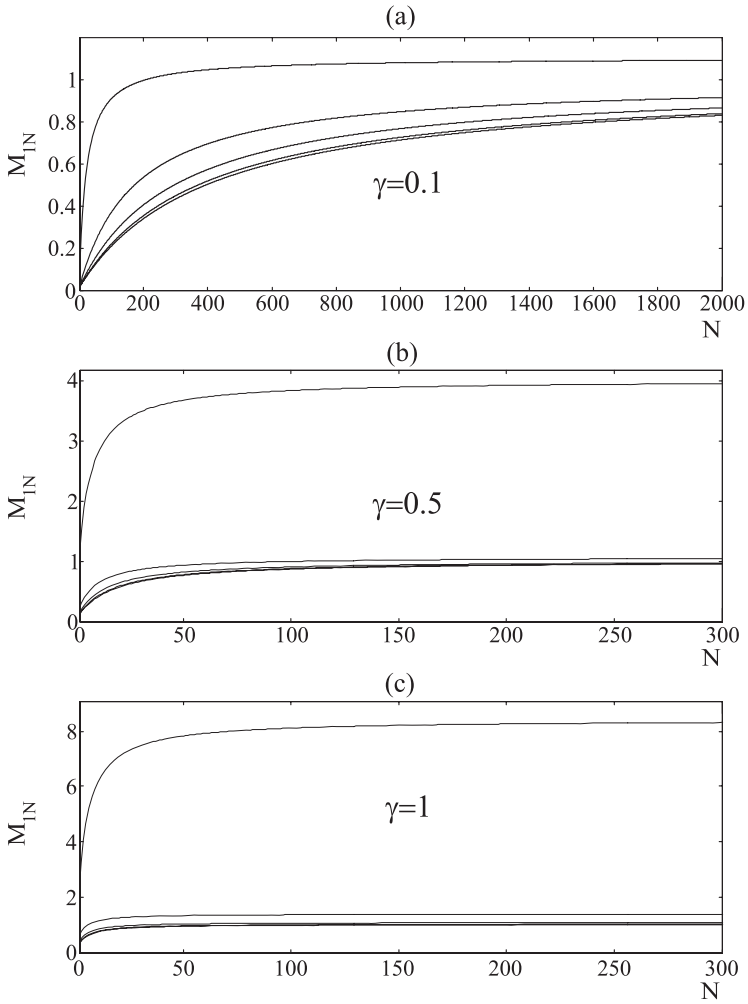

Figure 4. The quantity $M_{1N} = N \times |Z_{1N}|^2/\gamma^2$ is reported as a function of N for $\gamma = 0.1$ (a), $\gamma = 0.5$ (b) and $\gamma = 1$ (c). Notice that the represented curves tend to a constant, i.e. Z_{1N} decreases as $1/N$.

In the limit of weak coupling, we expect

$$B_{1N} \approx \gamma^2 \left[Q^2\right]_{1N} = \gamma^2 \sum_j Q_{1j} Q_{jN} \approx \gamma^2 N Q_{11}.$$

This suggests a linear increase of the incoherent contribution, for small N, at least in the weak (or intermediate) dephasing limit.

For large N, the expected behaviour of B_{1N} is a decrease as $1/N$. This can be analysed numerically as follows:

$$B_{1N} = \gamma^2 \left[Q \frac{1}{1-\gamma^2 Q} Q \right]_{1N} = \gamma^2 \sum_{ij} Q_{1i} \left(\frac{1}{1-\gamma^2 Q} \right)_{ij} Q_{jN}.$$

Due to the exponential decay of the Q_{1N} matrix element, the long-range behaviour of B_{1N} is

determined by the behaviour of the inverse matrix element

$$Z_{1N} = \gamma^2 \left[\frac{1}{1 - \gamma^2 Q} \right]_{1N}.$$

In figure 4, the behaviour of $M_{1N} = N|Z_{1N}|/\gamma^2$ for different energies and electron–phonon coupling strength is reported, and the algebraic decrease $1/N$ of the incoherent term is verified.

6. Conclusions

We have adopted the nonequilibrium Keldysh Green's function in the tight-binding formalism to evaluate the effect of disorder induced on the conductance by electron–phonon scattering active in a strand of a perfect infinite chain. The phonon scattering is described by the retarded, advanced, lesser and greater self-energy operators $\Sigma^{A,R,>,<(\mathrm{ph})}$, while the coupling of the central device to the leads is described by the self-energy operators $\Sigma^{A,R,>,<(\mathrm{leads})}$. In contrast to the other methods employed in the theory of disorder, in which statistical averages are performed on a suitably high number of disordered configurations, within the Keldysh theory disorder averages are automatically encompassed in the Dyson and kinetic equations of the adopted many-body model, in our case the self-consistent Born approximation.

By means of numerical simulations and analytic considerations we have provided a sound description of the coherent and incoherent contributions to the total conductance of the device. In particular we have recovered the expected decreasing exponential behaviour of the coherent term with strand length; but in addition we have evidenced for the incoherent term a linear growth for small N and a $1/N$ decrease for large N. These results should also contribute to a better understanding of phonon dephasing effects in realistic low-dimensional nanostructures, and for more sophisticated models of disorder, described by the full set of retarded, advanced, lesser and greater self-energies and Green's functions.

Acknowledgments

This work has been supported by Scuola Normale Superiore, and by National Enterprise for Nanoscience and Nanotechnology (NEST).

References

[1] Datta S 1990 *J. Phys.: Condens. Matter* **2** 8023
[2] Ferry D K and Goodnick S M 1997 *Transport in Nanostructures* (Cambridge: Cambridge University Press)
[3] Lin J J and Bird J P 2002 *J. Phys.: Condens. Matter* **14** R501
[4] Paulsson M, Frederiksen T and Brandbyge M 2005 *Phys. Rev.* B **72** 201101
[5] Bihary Z and Ratner M 2005 *Phys. Rev.* B **72** 115439
[6] Svizhenko A and Anantram M P 2005 *Phys. Rev.* B **72** 085430
[7] Pecchia A and Di Carlo A 2004 *Rep. Prog. Phys.* **67** 1497
[8] Emberly E G and Kirczenow G 2000 *Phys. Rev.* B **61** 5740
[9] Wu B H and Cao J C 2004 *J. Phys.: Condens. Matter* **16** 8285
[10] Das M P and Green F 2005 *J. Phys.: Condens. Matter* **17** V13
[11] Ness H 2006 *J. Phys.: Condens. Matter* **18** 6307
[12] Metalidis G and Bruno P 2006 *Phys. Rev.* B **73** 113308
[13] Imry Y and Landauer R 1999 *Rev. Mod. Phys.* **71** S306
[14] Büttiker M 1985 *Phys. Rev.* B **32** 1846
[15] Antonyuk V B, Mal'shukov A G, Larsson M and Chao K A 2004 *Phys. Rev.* B **69** 155308
[16] Jean N and Sanvito S 2006 *Phys. Rev.* B **73** 094433
[17] de la Vega L, Martín-Rodero A, Agraït N and Levi Yeyáti A 2006 *Phys. Rev.* B **73** 075428

[18] Kadanoff L P and Baym G 1962 *Quantum Statistical Mechanics* (New York: Benjamin)
[19] Keldysh L V 1964 *Zh. Éksp. Teor. Fiz.* **47** 1515
Keldysh L V 1965 *Sov. Phys.—JEPT* **20** 1018 (Engl. Transl.)
[20] Pastawski H M 1991 *Phys. Rev.* B **44** 6329
[21] Lake R and Datta S 1992 *Phys. Rev.* B **45** 6670
[22] Lake R, Klimeck G, Bowen R C and Jovanovic D 1997 *J. Appl. Phys.* **81** 7845
[23] Hyldgaard P, Hershfield S, Davies J H and Wilkins J W 1994 *Ann. Phys.* **236** 1
[24] Zagoskin A M 1998 *Quantum Theory of Many-Body Systems* (New York: Springer)
[25] Haug H and Jahuo A-P 1996 *Quantum Kinetics in Transport and Optics of Semiconductors* (Berlin: Springer)
[26] Wacker A and Hu B Y 1999 *Phys. Rev.* B **60** 16039
[27] Anderson P W 1958 *Phys. Rev.* **109** 1492
[28] Kramer B and MacKinnon A 1993 *Rep. Prog. Phys.* **56** 1469
[29] Caroli C, Combescot R, Nozières P and Saint-James D 1971 *J. Phys. C: Solid State Phys.* **4** 916
Caroli C, Combescot R, Nozières P and Saint-James D 1972 *J. Phys. C: Solid State Phys.* **5** 21
[30] Langreth D C 1976 *Linear and Nonlinear Electron Transport in Solids* ed J T Devreese and V E Van Doren (New York: Plenum)
[31] Bullett D W, Haydock R, Heine V and Kelly M J 1980 *Solid State Physics* vol 35, ed H Ehrenreich, F Seitz and P Turnbull (New York: Academic)
[32] Grosso G and Pastori Parravicini G 2000 *Solid State Physics* (London: Academic)
[33] Economou E N 1983 *Green's Function in Quantum Physics* (New York: Springer)